Circulation Journal
Official Journal of the Japanese Circulation Society
http://www.j-circ.or.jp

REVIEW

Optical Coherence Tomography
– 15 Years in Cardiology –

Taishi Yonetsu, MD; Brett E. Bouma, PhD; Koji Kato, MD, PhD;
James G. Fujimoto, PhD; Ik-Kyung Jang, MD, PhD

Since its invention in the late 1990s, intravascular optical coherence tomography (OCT) has been rapidly adopted in clinical research and, more recently, in clinical practice. Given its unprecedented resolution and high image contrast, OCT has been used to visualize plaque characteristics and to evaluate the vascular response to percutaneous coronary intervention. In particular, OCT is becoming the standard modality to evaluate in vivo plaque vulnerability, including the presence of lipid content, thin fibrous cap, or macrophage accumulation. Furthermore, OCT findings after stent implantation, such as strut apposition, neointimal hyperplasia, strut coverage, and neoatherosclerosis, are used as surrogate markers of the vascular response. New applications for OCT are being explored, such as transplant vasculopathy or non-coronary vascular imaging. Although OCT has contributed to cardiovascular research by providing a better understanding of the pathophysiology of coronary artery disease, data linking the images and clinical outcomes are lacking. Prospective data are needed to prove that the use of OCT improves patient outcomes, which is the ultimate goal of any clinical diagnostic tool. (*Circ J* 2013; **77:** 1933–1940)

Key Words: Coronary artery disease; Optical coherence tomography; Percutaneous coronary intervention

Since intravascular ultrasound (IVUS) was introduced in the early 1990s,[1,2] it has been used not only as an adjunctive device to percutaneous coronary interventions (PCI), but also as a research tool to evaluate vessel structure in detail. Although IVUS has helped broaden our understanding of coronary artery structure, its limited spatial resolution does not allow for the assessment of microstructures, which is important for identification of vulnerable plaques. Optical coherence tomography (OCT) is analogous to ultrasound, except that it generates images by measuring the echo time delay and magnitude of backscattered light instead of sound.[3] OCT was developed by Huang et al at the Massachusetts Institute of Technology and demonstrated for ex vivo imaging of the retina and atherosclerotic plaque in 1991.[3] A related concept to OCT was also independently proposed by Tanno et al in Japan in 1991.[4] OCT enables "optical biopsy", imaging tissue structure and pathology in situ and in real time. It has become a standard imaging modality in clinical ophthalmology, where it is used for the diagnosis of retinal disease, assessing disease progression and response to therapy.[5] The possibility of using OCT intravascularly was first suggested in 1996 by Brezinski et al in an ex vivo imaging study that demonstrated the ability of OCT to resolve the thin intimal cap layers that are associated with unstable plaques.[6] A prototype OCT imaging catheter using fiber optics was developed and demonstrated for imaging vascular structure ex vivo,[7] as well as for in vivo endoscopic imaging in animals.[8] In 1998 we established the first cardiac OCT research group at the Massachusetts General Hospital (MGH) to explore the clinical applications of OCT. In this review we will summarize the steps taken to bring this technology from bench to bedside over the past 15 years.

Ex Vivo Validation Studies

First, we performed ex vivo validation studies of OCT images in comparison with histological assessment of autopsy specimens. OCT images correlated with histology in 357 atherosclerotic arterial segments from 90 cadavers. From these data, we established the OCT definitions of fibrous, fibrocalcific, and lipid-rich plaques (**Figure 1**). We also demonstrated a high sensitivity and specificity of these criteria (90–98%) and high reproducibility between 2 observers.[9] In addition to plaque characterization, different types of intraluminal thrombus (red thrombus and white thrombus) were reported.[10] In a series of ex vivo studies, we reported that macrophage accumulation could be visualized by OCT.[11] Pathologically, infiltration and accumulation of foamy macrophages is an essential process in the development of vulnerable plaques.[12] Although it is impossible for IVUS to visualize macrophages (20–30 μm), OCT can identify accumulated macrophages as bright spots with heterogeneous signal intensity. Normalized standard deviation (NSD) calculated from the OCT signal intensity within the fibrous cap

Received May 23, 2013; accepted May 25, 2013; released online July 12, 2013
Cardiology Division (T.Y., K.K., I.-K.J.), Wellman Center for Photomedicine (B.E.B.), Massachusetts General Hospital and Harvard Medical School, Boston, MA; Department of Electrical Engineering and Computer Science and Research Laboratory of Electronics, Massachusetts Institute of Technology, Cambridge, MA (J.G.F.), USA
Mailing address: Ik-Kyung Jang, MD, PhD, Cardiology Division, Massachusetts General Hospital, GRB 800, 55 Fruit Street, Boston, MA, USA. E-mail: ijang@partners.org
ISSN-1346-9843 doi:10.1253/circj.CJ-13-0643.1

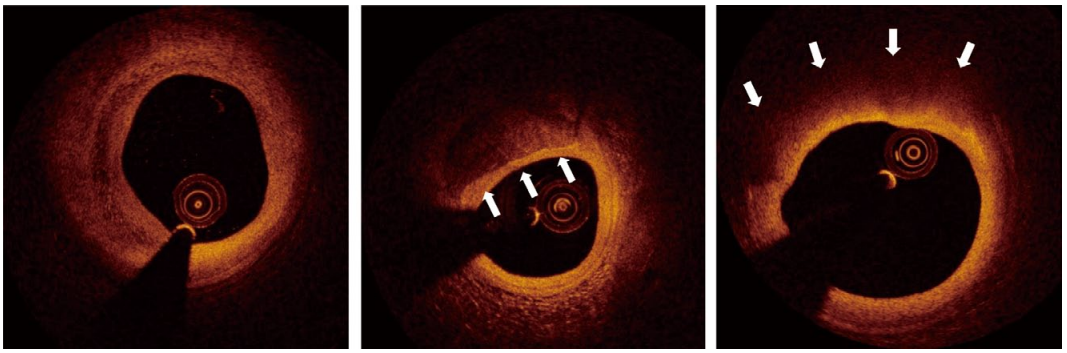

Figure 1. Plaque characterization by optical coherence tomography. Fibrous plaque is characterized by homogeneous, signal-rich region (**Left**). Fibrocalcific plaques are identified by well-delineated, signal-poor regions with sharp borders (arrows, **Middle**). Lipid is characterized by signal-poor region with diffuse borders (arrows, **Right**).

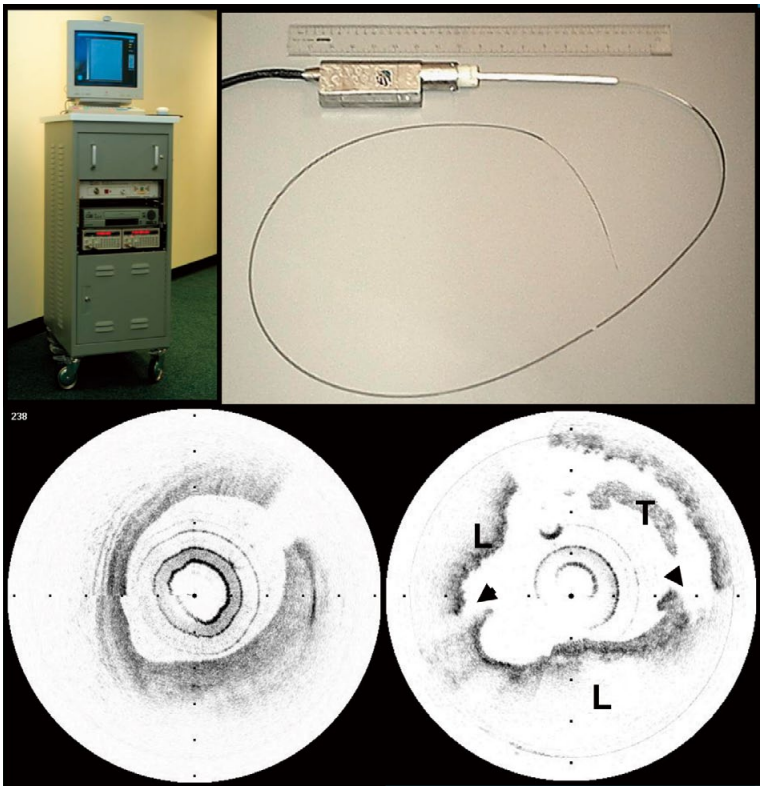

Figure 2. Proto-type optical coherence tomography (OCT) system (**Upper left**) and catheter (**Upper right**) used for the first human study. OCT could differentiate fibrous plaque (**Lower left**) and ruptured plaque (**Lower right**).

correlated closely with the percent area of $CD68^+$ cells determined by histology.[11] Although the potential quantification of macrophages by OCT raised significant interest, these findings were based on data obtained with a prototype OCT device and need to be verified with current commercial OCT instruments.

One of the most important capabilities of intracoronary OCT is the measurement of fibrous cap thickness and identification of thin cap fibroatheroma (TCFA). Pathologically, TCFA is defined as a plaque with advanced atherosclerosis showing a large necrotic core and a thin fibrous cap overlying inflammatory cell infiltration, which has been recognized as a hallmark of vulnerable plaque.[12] An ex vivo study demonstrated an excellent correlation between OCT and histologically measured fibrous cap thickness (r=0.90) in 35 lipid-rich plaques collected from 102 coronary segments in 38 human cadavers.[13] OCT is the only histologically validated modality that can measure fibrous cap thickness, and has become the standard in vivo imaging modality for identifying TCFA.

First-in-Man Study

Based on the promising data from the experimental studies, our group at MGH performed a first-in-man study in 2002 to evaluate the feasibility of using OCT to visualize plaque com-

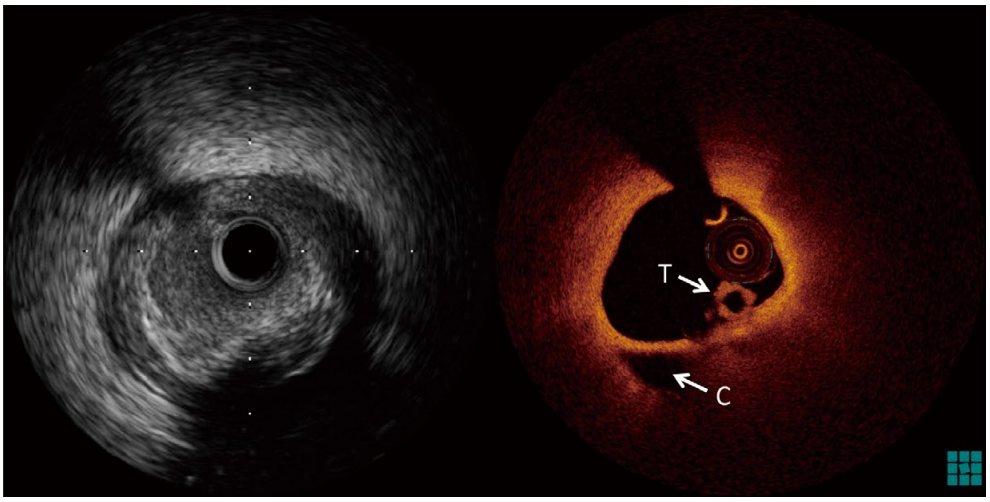

Figure 3. Comparison of intravascular ultrasound (IVUS) and optical coherence tomography (OCT). Matched images of IVUS (**Left**) and OCT (**Right**) of the culprit lesion in a patient with ST-elevation myocardial infarction. OCT clearly visualizes white thrombus (T) attached to the surface of a lipid-rich plaque with cavity (C), which can not be delineated by IVUS.

ponents in the coronary arteries of living humans.[14] The OCT instrument was a prototype developed at MGH and the OCT catheter was a modified 3.2F IVUS catheter (**Figure 2**). A single-mode optical fiber was inserted through the IVUS core and the distal end had a miniature gradient index lens and a micro prism to focus the OCT optical beam. Because of the limited image acquisition rate with this prototype OCT system, 8–10 ml of saline was intermittently flushed through the guiding catheter to clear the blood and obtain images of the arterial wall. In total, 17 lesions from 10 patients were imaged by both IVUS and OCT. That study demonstrated the potentially superior diagnostic ability of OCT over IVUS for the detection of various plaque components.[14]

In a subsequent study, we analyzed the culprit lesions of ST-elevation myocardial infarction (STEMI), non-ST-elevation acute coronary syndrome (NSTE-ACS), and stable angina pectoris (SAP) with OCT.[15] Of the 69 patients enrolled in the study, sufficient image quality was obtained in 57 (20 STEMI, 20 NSTE-ACS, and 17 SAP). TCFA, defined as a plaque with >90 degrees of lipid and <65 μm of fibrous cap thickness by OCT, was more frequently observed in STEMI and NSTE-ACS patients than in SAP patients (72%, 50%, and 20%, respectively, P=0.012); moreover, the fibrous cap was thinner in STEMI and NSTE-ACS than in SAP patients (47.0 μm, 53.8 μm, and 102.6 μm, respectively, P=0.034). This was the first in vivo study to demonstrate significant differences in plaque characteristics depending on the clinical presentation. In this first-in-man study, we confirmed the safety and feasibility of intracoronary OCT.

Advances in Imaging Speed

The first-in-man studies demonstrated the ability of OCT to visualize clinically relevant intravascular pathology, but the early OCT technology had limiting imaging speed. Because blood attenuates light by optical scattering, proximal occlusion, saline or contrast agent flushing was required in order to dilute the hematocrit during imaging. The resulting ischemia and limitations on the volumes of injected saline or contrast, combined with the limited image acquisition speed, meant that limited locations in the coronary arteries could be imaged. Increasing the OCT imaging speed was important for clinically practical intravascular imaging.

The first-generation OCT technology was based on "time domain" detection of optical echoes. In time domain detection, near-infrared light is focused onto the tissue and the echo time delay of the backscattered light is measured using an interferometer with a mechanically scanned reference path. Echoes of light are measured sequentially, 1 at a time, as the reference path is scanned. However, detection methods that operate in the "Fourier domain" enabled dramatic improvements in sensitivity and imaging speed. These methods are also known as "swept source OCT" or "optical frequency-domain imaging (OFDI)". Fourier domain detection operates by using an interferometer with a frequency swept laser.[16,17] Echoes of light from the tissue are interfered with by light from a stationary reference path and the echo delay generates an interferometer output with a frequency that is proportional to the echo delay. Fourier domain detection encodes spatial position as in frequency, somewhat analogous to MRI, and it has the advantage that it measures all of the echoes simultaneously, resulting in a dramatic improvement in sensitivity and imaging speed. The sensitivity and speed advantages were independently highlighted by 3 different research groups in 2003.[18–20] These advances enabled OCT imaging speeds to be increased by more than 10-fold, making intravascular imaging clinically practical.

Technology Translation and Commercial Development

In parallel to research advances, translation and commercial development are important in order to enable widespread access to new technology by the clinical community. LightLab Imaging, Inc (Westford, MA, USA) was founded in 1998 as an MIT startup in a joint venture with Carl Zeiss Meditec. LightLab was acquired by Goodman Ltd in 2002 and later sold to St. Jude Medical in 2011. LightLab introduced the M2 imaging system in Europe in 2002. This first-generation OCT in-

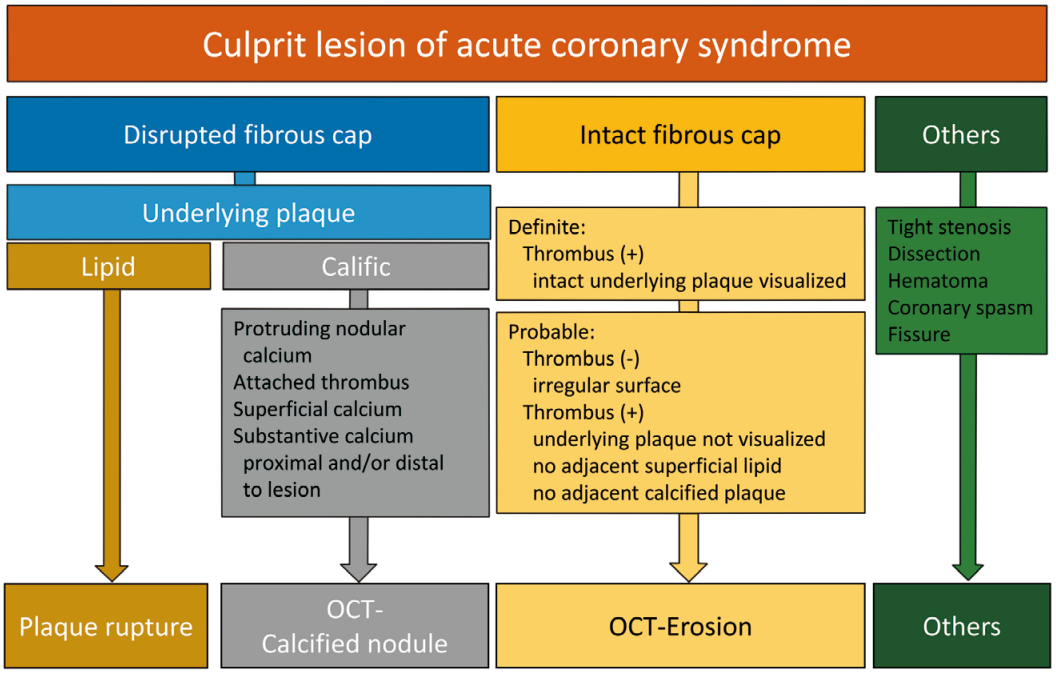

Figure 4. Definition of plaque erosion and calcified nodules according to optical coherence tomography (OCT). Definite erosion is defined as a lesion with thrombus that allows for visualization of the entire underlying intact plaque. Probable erosion is defined if the lesion has an irregular surface in the absence of thrombus or if the intraluminal thrombus does not allow for clear visualization of underlying plaque, and superficial lipid and substantial calcification can be ruled out. A calcified nodule is defined as a lesion with a disrupted fibrous cap overlying protruding nodular calcium showing attached thrombus, superficial calcium, and substantial calcification in the proximal and distal adjacent regions.

strument used time domain detection and operated with 15 frames per second (200 axial scans per frame) using saline flushing and occlusion. The M3 system improved imaging speeds to 20 frames/s (240 axial scans/frame) and was introduced in Japan in 2007. The C7^{XR} ™ system used Fourier domain detection to achieve imaging speeds of 100 frames/s (500 axial scans/frame) and was introduced in 2010. This was a 10-fold increase in imaging speed, which enabled higher frame rates for improved pull-back speeds and arterial coverage, as well as increased axial scan density for improved image quality. These high imaging speeds enabled occlusion-free imaging using contrast agent injection to dilute hematocrit. The most recent generation of OCT systems (Ilumien™ and Illumien Optis™ OCT Intravascular Imaging Systems, St. Jude Medical, St. Paul, MN, USA) provides integrated FFR and OCT with a fast pull-back speed (20–36 mm/s) and longer pull-back length (50–75 mm), which does not require vessel occlusion. These improvements in imaging speeds and system performance promise to enable a wide range of clinical studies

In Vivo Plaque Characterization

OCT has contributed to clarifying the pathophysiology of coronary atherosclerosis, which has been challenging for other in vivo imaging modalities because of either limited image resolution or poor image contrast (**Figure 3**). By maximizing the advantages of OCT, plaque characteristics relevant to ACS have been extensively explored.[21–25] Macrophage accumulation is thought to weaken the fibrous cap overlying the necrotic core and lead to plaque rupture.[26,27] Macrophage density, estimated by the NSD of the OCT signal, is significantly higher in ACS patients compared with SAP patients.[21] Expansive remodeling is known to be associated with ACS.[12,28,29] In our OCT and IVUS study,[30] TCFA was more frequently observed in lesions with positive remodeling than in those with intermediate or negative remodeling (80%, 38.5%, and 5.6%, respectively, P<0.001). Moreover, the involved lipid quadrants correlated with a remodeling index as determined by IVUS. Intraplaque neovascularization, which is considered to be a driver of plaque instability, is visualized by OCT as a vesicular structure within the plaque, and also referred to as microchannels, microvessels, or intimal vasculature. Neovascularization visualized with OCT has been associated with a thin fibrous cap,[31] poor responsiveness to statin therapy,[32] and plaque progression,[33] thus supporting concepts derived from pathology. OCT is a unique in vivo imaging modality that enables visualization of the fibrous cap of atheromatous plaque. With the use of OCT, the morphology of fibrous cap disruption has been studied. Tanaka et al reported that shoulder-type rupture was more frequently observed in patients developing ACS on exertion than in those developing it at rest.[22] Moreover, plaque rupture was more frequent in STEMI patients than in NSTE-ACS (70% vs. 47%, P=0.033), and cap disruption tended to be directed against the coronary flow in STEMI patients.[25] Fibrous cap thickness is one of the most critical determinants of plaque rupture susceptibility.[12] The widely accepted cut-off point for rupture-prone plaque, 65 μm, was obtained from a pathological study[34] in which the thinnest fibrous cap thickness was measured in 41 ruptured plaques causing sudden cardiac death (95th percentile value, 65 μm).

In an in vivo OCT study comparing ruptured plaque with non-ruptured lipid-rich plaque, a fibrous cap thickness <80 μm at its thinnest point was the threshold for ruptured plaque, which is consistent with expected tissue shrinkage ranging from 10% to 20% during histopathologic processing.[35,36]. In addition to the culprit lesions, nonculprit lesions of ACS have also been studied by OCT. Nonculprit lesions of ACS show more features of vulnerability, including greater lipid amount, thinner fibrous cap thickness, and more neovascularization close to the lumen compared with the non-target lesions of SAP.[37] These results suggest that ACS is a systemic, pan-vascular disease rather than a focal phenomenon of the coronary arteries. Moreover, plaque characterization by OCT has been used in other clinical settings such as diabetes mellitus and chronic kidney disease.[38,39]

Pathogenesis of ACS

As just described, one of the greatest advantages of OCT is the ability to obtain precise plaque characterization, including assessment of microstructures such as fibrous cap, macrophage accumulation, and neovascularization. As these findings are relevant to plaque instability, OCT may be the ideal modality for assessing the pathophysiology of ACS.[40] Although ruptured plaque has been recognized as the primary cause of ACS, previous pathological studies demonstrated that other causes, such as plaque erosion and calcified nodules, account for approximately 20% of sudden cardiac deaths and 25–40% of acute coronary thromboses.[12,41,42] Recently, more attention has been paid to these potential mechanisms of ACS. Pathologically, plaque erosion is defined as thrombus formation on the surface of a plaque with denudation of the endothelial layer,[12] and a calcified nodule is defined as a heavily calcified plaque with loss or dysfunction of the endothelium, resulting in loss of the fibrous cap over the nodular calcium.[12] Some OCT studies attempted to define the features of plaque erosions used the same definition as pathology[43] or simply defined plaque erosion as thrombus formation with an intact fibrous cap. However, the limitations of OCT resolution and penetration do not allow for the visualization of endothelial cells (<10 μm) or for the detection of the fibrous cap behind a massive thrombus.[44] Therefore, we proposed an OCT definition of plaque erosion and calcified nodules in collaboration with pathologists. Our definition classifies the culprit lesions of ACS into plaque rupture, calcified nodules, definite erosion, probable erosion, and an unclassified (other) group (**Figure 4**).[45] With this definition, we analyzed a total of 126 ACS culprit lesions with OCT and found that 55 (44%) showed plaque rupture, 39 (23%) had OCT-identified erosion (23 definite erosions and 16 probable erosions), and 10 (8%) had OCT-defined calcified nodules. Patients with erosion were younger and more frequently experienced NSTE-ACS rather than STEMI. These data were identical to those from pathology, suggesting that patients with OCT-defined erosion may closely resemble patients with pathologically-defined erosion. Given the different mechanisms and different patient backgrounds leading to ACS, it is important to consider different therapeutic strategies for these patients. The current therapeutic strategy for ACS patients, especially for those with STEMI, was designed under the premise that coronary thrombosis occurred subsequent to plaque rupture. However, if we could identify the cases of ACS caused by erosion or calcified nodules, we might be able to treat them with antithrombotic therapy instead of stenting, because those lesions theoretically have less occlusive plaque underneath the thrombus and thus could be dissolved with antithrombotic agents. Prospective studies are warranted for this possible new paradigm.

Complications in PCI

OCT is much more sensitive than IVUS to detect mechanical complications caused by stent placement onto the vessel wall, such as tissue protrusion, dissection at the edge, and incomplete stent apposition.[46,47] Several single-center studies have been published regarding stent complications detected by OCT.[47–50] Tissue protrusion, which includes prolapsed tissue components and intrastent thrombus, is detectable by OCT in the majority of cases, ranging from 40% to 95% depending on the underlying plaque type and clinical presentation.[46,49,50] Stent edge dissection is also detected frequently, its incidence varying according to plaque type at the stent edge and clinical characteristics.[48,51] Moreover, the amount of lipid at the proximal stent edge has been associated with periprocedural cardiac marker elevation.[52] Although OCT can not image through the optically opaque stent struts, strut apposition can be assessed by determining metal and polymer thickness relative to the lumen.[53] Incomplete apposition is also common immediately after stenting, with its incidence varying from 10% to 60% according to underlying plaque characteristics.[46,50] Previous studies using serial OCT examinations[47,54] have reported that most edge dissections and intramural protrusions have resolved at the 6–8-month follow-up OCT examination.[41,48] Dissolution of incomplete stent apposition depends on the distance between the strut and lumen.[54] Guagliumi et al demonstrated the association of malapposition and uncovered struts with late stent thrombosis.[55] By retrospectively comparing the OCT findings of 18 stents with late thrombosis and 36 matched cases, they found that malapposed and uncovered struts were more frequently observed in cases of late thrombosis. In recent years, OCT has been used in a number of studies assessing the coverage and apposition of stents as surrogate markers of the vascular response to stent implantation.[56–58] Nevertheless, no prospective data assessing the clinical effect of these minor complications have been reported. Given the low incidence of adverse events after contemporary PCI, data from many prospective cases will be needed to achieve statistically significant results for the clinical implications of these minor complications.

Neointimal Hyperplasia and Neoatherosclerosis Inside the Stents

OCT has been used to evaluate the tissue characteristics of neointimal hyperplasia in addition to the extent and amount of neointima.[59,60] In general, neointimal tissue is categorized according to its appearance into homogeneous, heterogeneous, and layered patterns as visualized by OCT.[59] It has been reported that the homogenous pattern represents tissue rich in smooth muscle cells, and the heterogeneous or layered pattern represents extracellular matrix, such as proteoglycans, in the low-signal regions.[61,62] Recently, pathological and OCT studies have shed light on the development of advanced atherosclerosis within neointima after stenting, which has been termed "neoatherosclerosis".[63,64] Takano et al reported the development of lipid-laden neointima more frequently in the late phase (>5 years) as compared with the early phase (<1 year) after bare metal stent (BMS) implantation;[63] theirs was the first description of neoatherosclerosis by OCT. Disruption of the fibrous cap and thrombus formation associated with neoatherosclerosis has been reported,[63,65] suggesting a potential mechanism of late stent thrombosis. Neoatherosclerosis

was also reported after drug-eluting stent (DES) implantation, especially in patients who presented with ACS caused by in-stent restenosis.[66] We investigated 138 stents with neointima (>100 μm) stratifying them into early (<9 months), intermediate (9–48 months), and delayed phases (>48 months), and compared the incidence of neoatherosclerosis between BMS and DES. Neoatherosclerosis was more frequent in DES than in BMS in both the early and intermediate phases, whereas no difference was observed in the delayed phase,[67] supporting the pathological data showing earlier development of neoatherosclerosis with DES.[64] Clinical predictors of neoatherosclerosis were also determined. Duration from stenting, DES, and current smoking habit were all independent predictors of neoatherosclerosis, and angiotensin-converting enzyme inhibitor (ACE-I) or angiotensin II receptor blocker (ARB) use was inversely associated, which suggests the protective effect of those agents on neointima formation.[68] Metallic stent implantation, including BMS and DES, has been the primary mode of PCI for more than 2 decades. However, there are remaining problems related to the vascular response to those "foreign" materials (polymer and metal). OCT is the best available in vivo imaging modality to evaluate these vascular responses, which in turn should help us find a solution.

Potential for Specific Indications

Alfonso et al reported OCT findings in patients with suspected spontaneous coronary dissection. Although spontaneous coronary dissection is rare, OCT clearly identified spontaneous coronary dissection with the appearance of double-lumen or hematoma.[69] Vessel structure visualization, especially the intimal tear initiating the dissection, is essential for appropriate management of spontaneous coronary dissection by sealing the tear with stent implantation.[69,70]

Cardiac allograft vasculopathy, which is a major cause of graft failure in heart transplant recipients, has also been investigated using OCT.[71] Although its diagnosis is challenging because of a lack of symptoms other than sudden cardiac death or heart failure, OCT may provide information that can lead to an early diagnosis of allograft vasculopathy. Another potentially important application of OCT is for the evaluation of the bioabsorbable scaffold. Since the Igaki-Tamai stent was introduced as the first bioabsorbable stent,[72] bioabsorbable scaffolds have been developed and become available in some parts of the world. As the scaffold degrades over time within the vessel wall, it is important to monitor the bioresorption process for a better understanding and further development of effective devices. OCT has been used to follow the process, which varies according to the progress of desorption into a box-like shape, bright spot, or black box.[73]

Furthermore, in addition to the coronary arteries, intravascular OCT has been used to visualize different peripheral arteries such as the carotid,[74] radial[75] and infra-inguinal.[76] Of note, OCT may provide new insights in the field of pulmonary hypertension (PH).[77] We have reported the OCT visualization of intimal thickening of the pulmonary artery in patients with PH;[78] the measurements of the vessel structure were validated in an ex vivo study.[79] In comparison with IVUS, OCT provides a clear image of vessel structures,[78] which can be a surrogate of pathological severity and may help improve the management of patients with PH.

MGH OCT Registry

As mentioned before, intracoronary OCT imaging has been used in both the clinical setting and clinical research for the past 15 years. Based on its high-resolution imaging performance and with the rapid development of the technology, OCT has contributed to our understanding of the in vivo pathophysiology of coronary artery disease and has aided in evaluating outcomes after stent implantation. Although some studies demonstrated its usefulness for the prediction of short-term outcomes after PCI,[80–82] there is as yet currently no convincing data showing that the use of OCT imaging improves clinical outcomes. Given that it is an invasive technique, it is difficult to conduct a large-scale, long-term, randomized controlled trial that would provide outcome-based evidence demonstrating the clinical efficacy of OCT imaging. To address this challenge, we created the MGH OCT Registry in 2009, which is a multicenter registry of patients undergoing OCT imaging of coronary arteries for any clinical indication. Currently, 20 sites across 6 countries (United States 5, Japan 4, Korea 5, Australia 2, China 2, and Singapore) participate in the Registry, which targets 3,000 cases with clinical follow-up of 5 years. We believe that the accumulated data in this Registry may be able to answer many of the unsolved questions, including the ultimate utility of OCT in the clinical setting.

Conclusions

OCT has been used for both clinical and research uses in cardiology for the past 15 years. With its unprecedented ability to visualize the detailed structure of the arterial wall, OCT has helped us to understand in vivo vascular biology. A larger, prospective study is warranted to definitely elucidate the clinical role of OCT.

Acknowledgments

The authors thank all the investigators, healthcare providers, and supporting staff at the participating institutions of the MGH OCT Registry for their generous contributions. We also thank all the fellows, the research nurse, and the data manager for providing excellent work in the core laboratory, and Russell Joye for his editorial expertise.

Disclosure

Dr IK Jang received a research grant and consulting fee from LightLab Imaging/St. Jude Medical.

References

1. Potkin BN, Bartorelli AL, Gessert JM, Neville RF, Almagor Y, Roberts WC, et al. Coronary artery imaging with intravascular high-frequency ultrasound. *Circulation* 1990; **81:** 1575–1585.
2. Tobis JM, Mallery J, Mahon D, Lehmann K, Zalesky P, Griffith J, et al. Intravascular ultrasound imaging of human coronary arteries in vivo: Analysis of tissue characterizations with comparison to in vitro histological specimens. *Circulation* 1991; **83:** 913–926.
3. Huang D, Swanson EA, Lin CP, Schuman JS, Stinson WG, Chang W, et al. Optical coherence tomography. *Science* 1991; **254:** 1178–1181.
4. Tanno N, Tsutomu I, Saeki A. Device for measuring light wave of a reflected image. Japanese Patent JP04174345. 1992.
5. Puliafito CA, Hee MR, Lin CP, Reichel E, Schuman JS, Duker JS, et al. Imaging of macular diseases with optical coherence tomography. *Ophthalmology* 1995; **102:** 217–229.
6. Brezinski ME, Tearney GJ, Bouma BE, Izatt JA, Hee MR, Swanson EA, et al. Optical coherence tomography for optical biopsy: Properties and demonstration of vascular pathology. *Circulation* 1996; **93:** 1206–1213.
7. Tearney GJ, Brezinski ME, Boppart SA, Bouma BE, Weissman N, Southern JF, et al. Catheter-based optical imaging of a human coronary artery. *Circulation* 1996; **94:** 3013.
8. Tearney GJ, Brezinski ME, Bouma BE, Boppart SA, Pitvis C, Southern JF, et al. In vivo endoscopic optical biopsy with optical coherence tomography. *Science* 1997; **276:** 2037–2039.
9. Yabushita H, Bouma BE, Houser SL, Aretz HT, Jang IK, Schlendorf

KH, et al. Characterization of human atherosclerosis by optical coherence tomography. *Circulation* 2002; **106:** 1640–1645.
10. Kume T, Akasaka T, Kawamoto T, Ogasawara Y, Watanabe N, Toyota E, et al. Assessment of coronary arterial thrombus by optical coherence tomography. *Am J Cardiol* 2006; **97:** 1713–1717.
11. Tearney GJ, Yabushita H, Houser SL, Aretz HT, Jang IK, Schlendorf KH, et al. Quantification of macrophage content in atherosclerotic plaques by optical coherence tomography. *Circulation* 2003; **107:** 113–119.
12. Virmani R, Kolodgie FD, Burke AP, Farb A, Schwartz SM. Lessons from sudden coronary death: A comprehensive morphological classification scheme for atherosclerotic lesions. *Arterioscler Thromb Vasc Biol* 2000; **20:** 1262–1275.
13. Kume T, Akasaka T, Kawamoto T, Okura H, Watanabe N, Toyota E, et al. Measurement of the thickness of the fibrous cap by optical coherence tomography. *Am Heart J* 2006; **152:** 755.e1–e4.
14. Jang IK, Bouma BE, Kang DH, Park SJ, Park SW, Seung KB, et al. Visualization of coronary atherosclerotic plaques in patients using optical coherence tomography: Comparison with intravascular ultrasound. *J Am Coll Cardiol* 2002; **39:** 604–609.
15. Jang IK, Tearney GJ, MacNeill B, Takano M, Moselewski F, Iftima N, et al. In vivo characterization of coronary atherosclerotic plaque by use of optical coherence tomography. *Circulation* 2005; **111:** 1551–1555.
16. Golubovic B, Bouma BE, Tearney GJ, Fujimoto JG. Optical frequency-domain reflectometry using rapid wavelength tuning of a Cr4+: Forsterite laser. *Optics Lett* 1997; **22:** 1704–1706.
17. Chinn SR, Swanson EA, Fujimoto JG. Optical coherence tomography using a frequency-tunable optical source. *Optics Lett* 1997; **22:** 340–342.
18. Choma MA, Sarunic MV, Yang CH, Izatt JA. Sensitivity advantage of swept source and Fourier domain optical coherence tomography. *Optics Express* 2003; **11:** 2183–2189.
19. de Boer JF, Cense B, Park BH, Pierce MC, Tearney GJ, Bouma BE. Improved signal-to-noise ratio in spectral-domain compared with time-domain optical coherence tomography. *Optics Lett* 2003; **28:** 2067–2069.
20. Leitgeb R, Hitzenberger CK, Fercher AF. Performance of Fourier domain vs. time domain optical coherence tomography. *Optics Express* 2003; **11:** 889–894.
21. MacNeill BD, Jang IK, Bouma BE, Iftimia N, Takano M, Yabushita H, et al. Focal and multi-focal plaque macrophage distributions in patients with acute and stable presentations of coronary artery disease. *J Am Coll Cardiol* 2004; **44:** 972–979.
22. Tanaka A, Imanishi T, Kitabata H, Kubo T, Takarada S, Tanimoto T, et al. Morphology of exertion-triggered plaque rupture in patients with acute coronary syndrome: An optical coherence tomography study. *Circulation* 2008; **118:** 2368–2373.
23. Tanimoto T, Imanishi T, Tanaka A, Yamano T, Kitabata H, Takarada S, et al. Various types of plaque disruption in culprit coronary artery visualized by optical coherence tomography in a patient with unstable angina. *Circ J* 2009; **73:** 187–189.
24. Kashiwagi M, Tanaka A, Kitabata H, Tsujioka H, Matsumoto H, Arita Y, et al. Relationship between coronary arterial remodeling, fibrous cap thickness and high-sensitivity C-reactive protein levels in patients with acute coronary syndrome. *Circ J* 2009; **73:** 1291–1295.
25. Ino Y, Kubo T, Tanaka A, Kuroi A, Tsujioka H, Ikejima H, et al. Difference of culprit lesion morphologies between ST-segment elevation myocardial infarction and non-ST-segment elevation acute coronary syndrome: An optical coherence tomography study. *JACC Cardiovasc Interv* 2011; **4:** 76–82.
26. Fuster V. Lewis A. Mechanisms leading to myocardial infarction: Insights from studies of vascular biology [Conner Memorial Lecture]. *Circulation* 1994; **90:** 2126–2146.
27. Lendon CL, Davies MJ, Born GV, Richardson PD. Atherosclerotic plaque caps are locally weakened when macrophages density is increased. *Atherosclerosis* 1991; **87:** 87–90.
28. Schoenhagen P, Ziada KM, Kapadia SR, Crowe TD, Nissen SE, Tuzcu EM. Extent and direction of arterial remodeling in stable versus unstable coronary syndromes: An intravascular ultrasound study. *Circulation* 2000; **101:** 598–603.
29. Nakamura M, Nishikawa H, Mukai S, Setsuda M, Nakajima K, Tamada H, et al. Impact of coronary artery remodeling on clinical presentation of coronary artery disease: An intravascular ultrasound study. *J Am Coll Cardiol* 2001; **37:** 63–69.
30. Raffel OC, Merchant FM, Tearney GJ, Chia S, Gauthier DD, Pomerantsev E, et al. In vivo association between positive coronary artery remodelling and coronary plaque characteristics assessed by intravascular optical coherence tomography. *Eur Heart J* 2008; **29:** 1721–1728.
31. Tian J, Hou J, Xing L, Kim SJ, Yonetsu T, Kato K, et al. Significance of intraplaque neovascularisation for vulnerability: Optical coherence tomography study. *Heart* 2012; **98:** 1504–1509.
32. Tian J, Hou J, Xing L, Kim SJ, Yonetsu T, Kato K, et al. Does neovascularization predict response to statin therapy? Optical coherence tomography study. *Int J Cardiol* 2012; **158:** 469–470.
33. Uemura S, Ishigami K, Soeda T, Okayama S, Sung JH, Nakagawa H, et al. Thin-cap fibroatheroma and microchannel findings in optical coherence tomography correlate with subsequent progression of coronary atheromatous plaques. *Eur Heart J*; **33:** 78–85.
34. Burke AP, Farb A, Malcom GT, Liang YH, Smialek J, Virmani R. Coronary risk factors and plaque morphology in men with coronary disease who died suddenly. *N Engl J Med* 1997; **336:** 1276–1282.
35. Yonetsu T, Kakuta T, Lee T, Takahashi K, Kawaguchi N, Yamamoto G, et al. In vivo critical fibrous cap thickness for rupture-prone coronary plaques assessed by optical coherence tomography. *Eur Heart J* 2011; **32:** 1251–1259.
36. Lee RM. A critical appraisal of the effects of fixation, dehydration and embedding of cell volume. *In*: Revel JP, Barnard T, Haggis GH, editors. Scanning electron microscopy. Chicago: AMF O'Hare, 1984; 61–70.
37. Kato K, Yonetsu T, Kim SJ, Xing L, Lee H, McNulty I, et al. Nonculprit plaques in patients with acute coronary syndromes have more vulnerable features compared with those with non-acute coronary syndromes: A 3-vessel optical coherence tomography study. *Circ Cardiovasc Imaging* 2012; **5:** 433–440.
38. Kato K, Yonetsu T, Kim SJ, Xing L, Lee H, McNulty I, et al. Comparison of nonculprit coronary plaque characteristics between patients with and without diabetes: A 3-vessel optical coherence tomography study. *JACC Cardiovasc Interv* 2012; **5:** 1150–1158.
39. Kato K, Yonetsu T, Jia H, Abtahian F, Vergallo R, Hu S, et al. Nonculprit coronary plaque characteristics of chronic kidney disease. *Circ Cardiovasc Imaging* 2013; **6:** 448–456.
40. Maurovich-Horvat P, Schlett CL, Alkadhi H, Nakano M, Stolzmann P, Vorpahl M, et al. Differentiation of early from advanced coronary atherosclerotic lesions: Systematic comparison of CT, intravascular US, and optical frequency domain imaging with histopathologic examination in ex vivo human hearts. *Radiology* 2012; **265:** 393–401.
41. Farb A, Burke AP, Tang AL, Liang TY, Mannan P, Smialek J, et al. Coronary plaque erosion without rupture into a lipid core: A frequent cause of coronary thrombosis in sudden coronary death. *Circulation* 1996; **93:** 1354–1363.
42. Arbustini E, Dal Bello B, Morbini P, Burke AP, Bocciarelli M, Specchia G, et al. Plaque erosion is a major substrate for coronary thrombosis in acute myocardial infarction. *Heart* 1999; **82:** 269–272.
43. Kubo T, Imanishi T, Takarada S, Kuroi A, Ueno S, Yamano T, et al. Assessment of culprit lesion morphology in acute myocardial infarction: Ability of optical coherence tomography compared with intravascular ultrasound and coronary angioscopy. *J Am Coll Cardiol* 2007; **50:** 933–939.
44. Vergallo R, Yonetsu T, Kato K, Jia H, Abtahian F, Tian J, et al. Evaluation of culprit lesions by optical coherence tomography in patients with ST-elevation myocardial infarction. *Int J Cardiol* 2013 February 13, doi:10.1016/j.ijcard.2013.01.041 [Epub ahead of print].
45. Jia H, Abtahian F, Aguirre AD, Lee S, Chia S, Lowe H, et al. In vivo diagnosis of plaque erosion and calcified nodule in patients with acute coronary syndrome by intravascular optical coherence tomography. *J Am Coll Cardiol* 2013 June 27, doi:10.1016/j.jacc.2013.05.071 [Epub ahead of print].
46. Bouma BE, Tearney GJ, Yabushita H, Shishkov M, Kauffman CR, DeJoseph Gauthier D, et al. Evaluation of intracoronary stenting by intravascular optical coherence tomography. *Heart* 2003; **89:** 317–320.
47. Kume T, Okura H, Miyamoto Y, Yamada R, Saito K, Tamada T, et al. Natural history of stent edge dissection, tissue protrusion and incomplete stent apposition detectable only on optical coherence tomography after stent implantation: Preliminary observation. *Circ J* 2012; **76:** 698–703.
48. Gonzalo N, Serruys PW, Okamura T, Shen ZJ, Garcia-Garcia HM, Onuma Y, et al. Relation between plaque type and dissections at the edges after stent implantation: An optical coherence tomography study. *Int J Cardiol* 2011; **150:** 151–155.
49. Gonzalo N, Serruys PW, Okamura T, Shen ZJ, Onuma Y, Garcia-Garcia HM, et al. Optical coherence tomography assessment of the acute effects of stent implantation on the vessel wall: A systematic quantitative approach. *Heart* 2009; **95:** 1913–1919.
50. Kubo T, Imanishi T, Kitabata H, Kuroi A, Ueno S, Yamano T, et al. Comparison of vascular response after sirolimus-eluting stent implantation between patients with unstable and stable angina pectoris: A serial optical coherence tomography study. *JACC Cardiovasc Imag-*

ing 2008; **1:** 475–484.
51. Zeglin-Sawczuk M, Jang IK, Kato K, Yonetsu T, Kim S, Choi SY, et al. Lipid rich plaque, female gender and proximal coronary stent edge dissections. *J Thromb Thrombolysis* 2013 February 2, doi:10.1007/s11239-013-0882-3 [Epub ahead of print].
52. Imola F, Occhipinti M, Biondi-Zoccai G, Di Vito L, Ramazzotti V, Manzoli A, et al. Association between proximal stent edge positioning on atherosclerotic plaques containing lipid pools and postprocedural myocardial infarction (from the CLI-POOL Study). *Am J Cardiol* 2013; **111:** 526–531.
53. Tanigawa J, Barlis P, Di Mario C. Intravascular optical coherence tomography: Optimisation of image acquisition and quantitative assessment of stent strut apposition. *EuroIntervention* 2007; **3:** 128–136.
54. Kawamori H, Shite J, Shinke T, Otake H, Matsumoto D, Nakagawa M, et al. Natural consequence of post-intervention stent malapposition, thrombus, tissue prolapse, and dissection assessed by optical coherence tomography at mid-term follow-up. *Eur Heart J Cardiovasc Imaging* 2013 January 4, doi:10.1093/ehjci/jes299 [Epub ahead of print].
55. Guagliumi G, Sirbu V, Musumeci G, Gerber R, Biondi-Zoccai G, Ikejima H, et al. Examination of the in vivo mechanisms of late drug-eluting stent thrombosis: Findings from optical coherence tomography and intravascular ultrasound imaging. *JACC Cardiovasc Interv* 2012; **5:** 12–20.
56. Kim JS, Fan C, Choi D, Jang IK, Lee JM, Kim TH, et al. Different patterns of neointimal coverage between acute coronary syndrome and stable angina after various types of drug-eluting stents implantation; 9-month follow-up optical coherence tomography study. *Int J Cardiol* 2011; **146:** 341–346.
57. Kim JS, Jang IK, Fan C, Kim TH, Park SM, Choi EY, et al. Evaluation in 3 months duration of neointimal coverage after zotarolimus-eluting stent implantation by optical coherence tomography: The ENDEAVOR OCT trial. *JACC Cardiovasc Interv* 2009; **2:** 1240–1247.
58. Kim JS, Kim BK, Jang IK, Shin DH, Ko YG, Choi D, et al. ComparisOn of neointimal coVerage betwEen zotaRolimus-eluting stent and everolimus-eluting stent using Optical Coherence Tomography (COVER OCT). *Am Heart J* 2012; **163:** 601–607.
59. Gonzalo N, Serruys PW, Okamura T, van Beusekom HM, Garcia-Garcia HM, van Soest G, et al. Optical coherence tomography patterns of stent restenosis. *Am Heart J* 2009; **158:** 284–293.
60. Hou J, Jia H, Liu H, Han Z, Yang S, Xu C, et al. Neointimal tissue characteristics following sirolimus-eluting stent implantation: OCT quantitative tissue property analysis. *Int J Cardiovasc Imaging* 2012; **28:** 1879–1886.
61. Kume T, Akasaka T, Kawamoto T, Watanabe N, Toyota E, Sukmawan R, et al. Visualization of neointima formation by optical coherence tomography. *Int Heart J* 2005; **46:** 1133–1136.
62. Nagai H, Ishibashi-Ueda H, Fujii K. Histology of highly echolucent regions in optical coherence tomography images from two patients with sirolimus-eluting stent restenosis. *Catheter Cardiovasc Interv* 2010; **75:** 961–963.
63. Takano M, Yamamoto M, Inami S, Murakami D, Ohba T, Seino Y, et al. Appearance of lipid-laden intima and neovascularization after implantation of bare-metal stents extended late-phase observation by intracoronary optical coherence tomography. *J Am Coll Cardiol* 2009; **55:** 26–32.
64. Nakazawa G, Otsuka F, Nakano M, Vorpahl M, Yazdani SK, Ladich E, et al. The pathology of neoatherosclerosis in human coronary implants bare-metal and drug-eluting stents. *J Am Coll Cardiol* 2011; **57:** 1314–1322.
65. Hou J, Qi H, Zhang M, Ma L, Liu H, Han Z, et al. Development of lipid-rich plaque inside bare metal stent: Possible mechanism of late stent thrombosis? An optical coherence tomography study. *Heart* 2010; **96:** 1187–1190.
66. Kang SJ, Mintz GS, Akasaka T, Park DW, Lee JY, Kim WJ, et al. Optical coherence tomographic analysis of in-stent neoatherosclerosis after drug-eluting stent implantation. *Circulation* 2011; **123:** 2954–2963.
67. Yonetsu T, Kim JS, Kato K, Kim SJ, Xing L, Yeh RW, et al. Comparison of incidence and time course of neoatherosclerosis between bare metal stents and drug-eluting stents using optical coherence tomography. *Am J Cardiol* 2012; **110:** 933–939.
68. Yonetsu T, Kato K, Kim SJ, Xing L, Jia H, McNulty I, et al. Predictors for neoatherosclerosis: A retrospective observational study from the optical coherence tomography registry. *Circ Cardiovasc Imaging* 2012; **5:** 660–666.
69. Alfonso F, Paulo M, Gonzalo N, Dutary J, Jimenez-Quevedo P, Lennie V, et al. Diagnosis of spontaneous coronary artery dissection by optical coherence tomography. *J Am Coll Cardiol* 2012; **59:** 1073–1079.
70. Alfonso F, Hernandez R, Goicolea J, Segovia J, Perez-Vizcayno MJ, Banuelos C, et al. Coronary stenting for acute coronary dissection after coronary angioplasty: Implications of residual dissection. *J Am Coll Cardiol* 1994; **24:** 989–995.
71. Hou J, Lv H, Jia H, Zhang S, Xing L, Liu H, et al. OCT assessment of allograft vasculopathy in heart transplant recipients. *JACC Cardiovasc Imaging* 2012; **5:** 662–663.
72. Tamai H, Igaki K, Kyo E, Kosuga K, Kawashima A, Matsui S, et al. Initial and 6-month results of biodegradable poly-l-lactic acid coronary stents in humans. *Circulation* 2000; **102:** 399–404.
73. Ormiston JA, Serruys PW, Regar E, Dudek D, Thuesen L, Webster MW, et al. A bioabsorbable everolimus-eluting coronary stent system for patients with single de-novo coronary artery lesions (ABSORB): A prospective open-label trial. *Lancet* 2008; **371:** 899–907.
74. Yoshimura S, Kawasaki M, Yamada K, Enomoto Y, Egashira Y, Hattori A, et al. Visualization of internal carotid artery atherosclerotic plaques in symptomatic and asymptomatic patients: A comparison of optical coherence tomography and intravascular ultrasound. *Am J Neuroradiol* 2012; **33:** 308–313.
75. Yonetsu T, Kakuta T, Lee T, Takayama K, Kakita K, Iwamoto T, et al. Assessment of acute injuries and chronic intimal thickening of the radial artery after transradial coronary intervention by optical coherence tomography. *Eur Heart J* 2010; **31:** 1608–1615.
76. Karnabatidis D, Katsanos K, Paraskevopoulos I, Diamantopoulos A, Spiliopoulos S, Siablis D. Frequency-domain intravascular optical coherence tomography of the femoropopliteal artery. *Cardiovasc Intervent Radiol* 2011; **34:** 1172–1181.
77. Fukumoto Y, Shimokawa H. Recent progress in the management of pulmonary hypertension. *Circ J* 2011; **75:** 1801–1810.
78. Hou J, Qi H, Zhang M, Meng L, Han Z, Yu B, et al. Pulmonary vascular changes in pulmonary hypertension: Optical coherence tomography findings. *Circ Cardiovasc Imaging* 2010; **3:** 344–345.
79. Li N, Zhang S, Hou J, Jang IK, Yu B. Assessment of pulmonary artery morphology by optical coherence tomography. *Heart Lung Circ* 2012; **21:** 778–781.
80. Lee T, Yonetsu T, Koura K, Hishikari K, Murai T, Iwai T, et al. Impact of coronary plaque morphology assessed by optical coherence tomography on cardiac troponin elevation in patients with elective stent implantation. *Circ Cardiovasc Intervent* 2011; **4:** 378–386.
81. Yonetsu T, Kakuta T, Lee T, Takahashi K, Yamamoto G, Iesaka Y, et al. Impact of plaque morphology on creatine kinase-MB elevation in patients with elective stent implantation. *Int J Cardiol* 2011; **146:** 80–85.
82. Porto I, Di Vito L, Burzotta F, Niccoli G, Trani C, Leone AM, et al. Predictors of periprocedural (type IVa) myocardial infarction, as assessed by frequency-domain optical coherence tomography. *Circ Cardiovasc Intervent* 2012; **5:** 89–96, S1–S6.